

AGLP: A Graph Learning Perspective for Semi-supervised Domain Adaptation

Houcheng Su
University of Macau

Mengzhu Wang *
Hebei University of Technology
dreamkily@gmail.com

Liang Yang
Hebei University of Technology
yangliang@vip.qq.com

Jiao Li
UESTC

Nan Yin
Zayed University of Artificial Intelligence
United Arab Emirates
yinnan8911@gmail.com

Li Shen *
Sun Yat-sen University
mathshenli@gmail.com

Abstract

In semi-supervised domain adaptation (SSDA), the model aims to leverage partially labeled target domain data along with a large amount of labeled source domain data to enhance its generalization capability for the target domain. A key advantage of SSDA is its ability to significantly reduce reliance on labeled data, thereby lowering the costs and time associated with data preparation. Most existing SSDA methods utilize information from domain labels and class labels but overlook the structural information of the data. To address this issue, this paper proposes a graph learning perspective (AGLP) for semi-supervised domain adaptation. We apply the graph convolutional network to the instance graph which allows structural information to propagate along the weighted graph edges. The proposed AGLP model has several advantages. First, to the best of our knowledge, this is the first work to model structural information in SSDA. Second, the proposed model can effectively learn domain-invariant and semantic representations, reducing domain discrepancies in SSDA. Extensive experimental results on multiple standard benchmarks demonstrate that the proposed AGLP algorithm outperforms state-of-the-art semi-supervised domain adaptation methods.

1. Introduction

Domain Adaptation (DA) [1, 18, 23] is a critical machine learning approach aimed at addressing the issue of training and test data originating from two related but distinct domains. These domains are typically referred to as the source domain and the target domain. In many practical applications, the source domain contains a wealth of la-

beled data, while the target domain may have only a few labels or even none at all. This discrepancy often leads to a significant drop in model performance when directly transferring a model from the source domain to the target domain. Much of the research has focused on Unsupervised Domain Adaptation (UDA). In UDA scenarios, researchers cannot access labels from the target domain, requiring models to rely on knowledge from the source domain and unlabeled data from the target domain for learning. In recent years, Semi-Supervised Domain Adaptation (SSDA) has emerged as a focal point of research. Unlike UDA, SSDA [1, 7, 21] allows researchers to access a small number of labeled samples in the target domain, providing the model with richer learning information. By combining the abundant labeled data from the source domain with the limited labeled data from the target domain, SSDA can more effectively capture the underlying structural relationships between the domains, thereby improving the model's performance and adaptability.

Prior SSDA methods can be broadly categorized into three groups: 1) statistical discrepancy minimization methods [1, 12], which utilize statistical regularizations to explicitly reduce the cross-domain distribution discrepancy; 2) adversarial learning methods [7, 21], which aim to learn domain-invariant representations across two domains using adversarial techniques; and 3) multi-task learning methods [14, 19], which focus on simultaneously learning multiple related tasks to share knowledge and improve the model's generalization ability.

Indeed, these SSDA methods have achieved some success, but the main technical challenge in SSDA lies in how to formally reduce the distribution discrepancy between different domains, typically the labeled source domain and the sparsely labeled target domain. There is little literature addressing the significant enhancement of the adaptation ca-

*Corresponding Author

pability of source-supervised classifiers, which is crucial for SSDA problems, as shown in Figure 2. To achieve classifier adaptation, He et al.[5] propose a novel classification-aware semi-supervised translator that effectively addresses the large gap between heterogeneous domains at the pixel level. Saito et al.[20] tackle the SSDA setting by proposing a novel Minimax Entropy approach that adversarially optimizes an adaptive few-shot model. The domain classifier is trained to determine whether a sample comes from the source domain or the target domain. The feature extractor is trained to minimize classification loss while maximizing domain confusion loss. Through the principled lens of adversarial training, it appears possible to obtain domain-invariant yet discriminative features. All of these methods overlook the aspect of learning domain-invariant features from the perspective of data structure.

To address the above issues, we propose an end-to-end Graph Convolutional Adversarial Network (GCAN) aimed at achieving semi-supervised domain adaptation. This network enhances adaptability by jointly modeling data structure and domain labels within a unified deep model. Inspired by graph neural networks, we construct a densely connected instance graph using the CNN features of samples, based on the similarity of their structural characteristics. Each node corresponds to the CNN features of a sample extracted by a standard convolutional network. Next, we apply a Graph Convolutional Network (GCN) to the instance graph, allowing structural information to propagate along the weighted graph edges that can be learned from the designed network. During the class centroid alignment process, we constrain the centroids of different classes to gradually move closer as iterations increase, enabling the learned representations to effectively encode class label information. This results in tighter embeddings for samples with the same category label in the feature space. Our model introduces a class alignment loss to achieve this goal and employs a moving centroid strategy to mitigate the influence of incorrect pseudo-labels. By modeling this alignment mechanism, the deep network can generate domain-invariant and highly discriminative semantic representations. The main contributions of this work can be summarized as follows.

- We propose a graph learning perspective (AGLP) by modeling data structure and domain label for semi-supervised domain adaptation. To the best of our knowledge, this is the first work to model graph information for semi-supervised domain adaptation.
- The proposed alignment mechanisms can learn domain-invariant and semantic representations effectively to reduce the domain discrepancy for SSDA.
- Extensive experimental results on several standard benchmarks demonstrate that the proposed AGLP algorithm performs favorably against state-of-the-art SSDA meth-

ods.

2. Method

2.1. Preliminaries

2.1.1 Semi-Supervised Domain Adaptation

Semi-Supervised Domain Adaptation (SSDA) aims to learn a classifier for the target domain, given labeled data $S = \{(x_i^s, y_i^s)\}_{i=1}^{N_s}$ from a source domain, along with both unlabeled data $U = \{x_i^u\}_{i=1}^{N_u}$ and labeled data $L = \{(x_i^l, y_i^l)\}_{i=1}^{N_l}$ from the target domain [1, 10, 20, 24]. The primary goal of SSDA is to leverage these data subsets to train a feature extractor $\mathcal{F}(\cdot)$ and a classifier $\mathcal{C}(\cdot)$, facilitating the migration of learned knowledge from the source domain to the target domain, while minimizing the risk of migration loss. SSDA can be viewed as a more flexible yet practical extension of Unsupervised Domain Adaptation (UDA)[15, 28], where some labeled data from the target domain is available. Typically, SSDA algorithms utilize a combination of three loss functions:

$$\mathcal{L}_{SSDA} = \mathcal{L}_s + \mathcal{L}_\ell + \mathcal{L}_u \quad (1)$$

where \mathcal{L}_s represents the loss from the source data, \mathcal{L}_ℓ and \mathcal{L}_u correspond to the losses from the labeled and unlabeled target data, respectively.

To train the model effectively using supervision from both the source and target domains, most existing SSDA methods [1, 10, 27] include the following standard cross-entropy loss for all labeled data:

$$\mathcal{L}_\ell = \mathcal{L}_{CE} = - \sum_{(x,y) \in \mathcal{S} \cup \mathcal{L}} y \log(p(x)) \quad (2)$$

In Eq. 2, (x, y) represents the data points and their corresponding labels from the source domain \mathcal{S} and the labeled target domain \mathcal{L} . The cross-entropy loss encourages the model to minimize the negative log-likelihood of the predicted probability $p(x)$ with respect to the true label y , thereby facilitating effective learning from both domains.

2.1.2 Cross-Domain Adaptive Clustering (CDAC)

Inspired by a recent well-known method CDAC [11], we consider improving model performance from the perspective of cross-domain clustering. CDAC introduce an adversarial adaptive clustering loss in SSDA to align target domain features by forming clusters and aligning them with source domain clusters. This loss computes pairwise feature similarities among target samples and ensures that samples with similar features share the same predicted class labels. Pairwise similarities are used to define binary pseudo-labels for sample pairs, $s_{ij} = 1$ for similar pairs and $s_{ij} = 0$ otherwise, based on the top- k ranked feature elements:

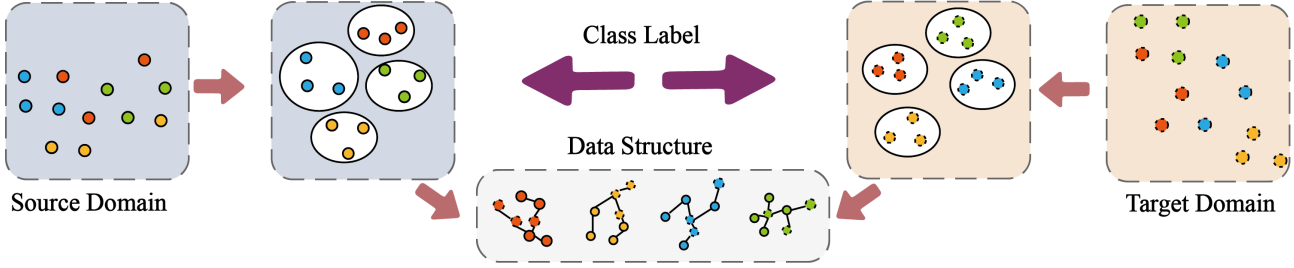


Figure 1. Illustration of our AGLP. The data structure is constructed to build graph information.

$$s_{ij} = \mathbf{1}\{\text{topk}(G(x_i^u)) = \text{topk}(G(x_j^u))\} \quad (3)$$

where $\text{topk}(\cdot)$ denotes the top- k indices of rank ordered feature elements and we set $k = 5$. And $\mathbf{1}\{\cdot\}$ is an indicator function.

The adversarial adaptive clustering loss \mathcal{L}_{AAC} is formulated as:

$$\mathcal{L}_{AAC} = - \sum_{i=1}^M \sum_{j=1}^M s_{ij} \log(P_i^T P_j) + (1 - s_{ij}) \log(1 - P_i^T P_j) \quad (4)$$

where M is the number of unlabeled target samples in each mini-batch and $P_i = p(x_i^u) = \sigma(F(G(x_i^u)))$ represents the prediction of an image x_i^u in the mini-batch. Also, $P_i' = p(x_i') = \sigma(F(G(x_i'))) indicates the prediction of a transformed image x_i' , which is an augmented version of x_i^u using a data augmentation technique. The inner product $P_i^T P_i'$ in Eq. 4 is used as a similarity score, which predicts whether image x_i^u and the transformed version of image x_i' share the same class label or not.$

To address the lack of labeled target samples, CDAC apply pseudo labeling, retaining high-confidence pseudo-labels to increase the number of labeled target samples. Pseudo labels are generated by feeding an unlabeled image x_j^u into the model, with the prediction $P_j = p(x_j^u)$ converted into a hard label $\tilde{y}_j^u = \arg \max(P_j)$. The final loss for pseudo-labeling is defined as:

$$\mathcal{L}_{PL} = - \sum_{j=1}^M \mathbf{1}\{\max(P_j) \geq \tau\} \tilde{y}_j^u \log(p_j'') \quad (5)$$

where $P_j'' = p(x_j'') = \sigma(F(G(x_j''))) denotes the model prediction of the transformed image x_j'' , and τ is a scalar confidence threshold that determines the subset of pseudo labels that should be retained for model training.$

To improve the input diversity of our model, we create two different transformed versions of each unlabeled image in the target domain to implement the adversarial adaptive clustering loss and the pseudo-labeling loss, respectively.

Therefore, CDAC employ a consistency loss, \mathcal{L}_{Con} , to keep the model predictions on these two transformed images consistent:

$$\mathcal{L}_{Con} = w(t) \sum_{j=1}^M \|P_j' - P_j''\|^2 \quad (6)$$

$w(t) = \nu e^{-5(1-\frac{t}{T})^2}$ is a ramp-up function used in with the scalar coefficient ν , the current time step t , and the total number of steps T in the ramp-up process. So, the \mathcal{L}_u is:

$$\mathcal{L}_u = \mathcal{L}_{Con} + \mathcal{L}_{PL} + \mathcal{L}_{AAC} \quad (7)$$

2.1.3 Source Label Adaptation (SLA)

In SSDA, accessing only a few labeled target instances can lead to overfitting. To mitigate this, SLA[27] employs a prototypical network (ProtoNet) to address the few-shot problem. Given a dataset, $\{(x_i, y_i)\}_{i=1}^N$ and a feature extractor f , the prototype of class k is defined as the mean of the feature representations for all samples belonging to class k :

$$c_k = \frac{1}{N_k} \sum_{i=1}^N \mathbf{1}\{y_i = k\} \cdot f(x_i). \quad (8)$$

The set of all class prototypes is denoted as $C_f = \{c_1, \dots, c_K\}$. A ProtoNet is defined using these class prototypes as:

$$P_{C_f}(x_i)_k = \frac{\exp(-d(f(x_i), c_k) \cdot T)}{\sum_{j=1}^K \exp(-d(f(x_i), c_j) \cdot T)} \quad (9)$$

where $d(\cdot)$ is a distance function in the feature space, typically Euclidean distance, and T controls the smoothness of the output distribution.

To adapt to the target domain, labeled target centers C_f^* are computed from labeled target data. The ProtoNet with labeled target centers $P_{C_f^*}$ serves as a label adaptation model. However, since the number of labeled target samples is limited, the ideal centers C_f^* should be estimated from both labeled and pseudo-labeled data. Pseudo centers

\tilde{C}_f are computed using pseudo-labels for the unlabeled target data, which are predicted as:

$$\tilde{y}_i^u = \arg \max_k g(x_i^u)_k \quad (10)$$

After deriving unlabeled target data with pseudo labels $\{(x_i^u, \tilde{y}_i^u)\}_{i=1}^{|U|}$, we can get pseudo centers C'_f by Eq. 8, and further define a ProtoNet with Pseudo Centers (PPC) $P_{C'_f}$ by Eq. 9.

The ProtoNet with pseudo centers (PPC) $\tilde{P}_{C'_f}$ better approximates the ideal centers. Then the updated source label is computed as:

$$y_i^s = (1 - \alpha) \cdot y_i^s + \alpha \cdot P_{\tilde{C}_f}(x_i^s) \quad (11)$$

The source label adaptation loss $\tilde{\mathcal{L}}_s$ replaces the standard cross-entropy loss for the source data:

$$\mathcal{L}_s = \tilde{\mathcal{L}}_s(g|S) = \frac{1}{|S|} \sum_{i=1}^{|S|} H(g(x_i^s), \tilde{y}_i^s) \quad (12)$$

The final loss function for SSDA with CDAC SLA is:

$$\mathcal{L}_{CDACSLA} = \tilde{\mathcal{L}}_s(g|S) + \mathcal{L}_{CE} + \mathcal{L}_{AAC} + \mathcal{L}_{PL} + \mathcal{L}_{Con} \quad (13)$$

2.2. Structure-aware Alignment

In traditional domain alignment mechanisms [13, 22], only global domain statistics are aligned, overlooking the inherent structural information in mini-batch samples. Previous research has focused primarily on modeling data structure in unsupervised domain adaptation (UDA) and has achieved promising results [17]. However, in the context of SSDA, there has been no solution addressing the structural information within mini-batch samples, despite its importance being demonstrated in UDA. To overcome this limitation in SSDA, we propose a structure-aware alignment mechanism that more effectively captures the structural relationships between mini-batch source and target samples.

Our approach begins by utilizing a Data Structure Analyzer (DSA) network to generate structural scores for mini-batch samples. These scores, together with the learned CNN features of the samples, are used to construct a densely connected instance graph. This instance graph is then processed using a Graph Convolutional Network (GCN) [9], which learns features that encode the structural information present in the data.

GCNs are designed to perform hierarchical propagation operations on graphs. Given an undirected graph with m nodes and a set of edges represented by an adjacency matrix $A \in \mathbb{R}^{k \times m}$, the graph convolution's linear transformation is expressed as a graph signal $G \in \mathbb{R}^{k \times m}$, where $G_i \in \mathbb{R}$

represents the feature of the i -th node. This is combined with a filter $W \in \mathbb{R}^{k \times c}$ for feature extraction.

$$\mathbf{Z} = \hat{\mathbf{D}}^{-\frac{1}{2}} \hat{\mathbf{A}} \hat{\mathbf{D}}^{-\frac{1}{2}} \mathbf{G}^T \mathbf{W} \quad (14)$$

In our method, the GCN is constructed by stacking multiple graph convolutional layers, each followed by a non-linear activation (e.g., ReLU). Given the adjacency matrix $\hat{A} = A + I$, where I is the identity matrix and $D_{ii} = \sum_j \hat{A}_{ij}$, the output of the GCN is a $c \times m$ matrix Z .

To build densely-connected instance graphs for GCN, the graph signal X is generated using a standard convolutional network:

$$G = \mathcal{F}(x_{\text{batch}}) \quad (15)$$

where x_{batch} represents mini-batch samples. The adjacency matrix \hat{A} is constructed using structure scores G_{sc} produced by a Data Structure Analyzer (DSA) network:

$$\hat{A} = G_{sc} G_{sc}^T, \quad (16)$$

where $G_{sc} \in \mathbb{R}^{w \times h}$, w is the batch size, and h is the dimension of the structure scores.

2.3. Class Centroid Alignment

Domain invariance and structure consistency do not necessarily guarantee discriminability. For example, features of the target class "laptops" may be mapped near features of the source class "screens" while still satisfying domain invariance. To address this, we draw inspiration from UDA [16], where class label information ensures that features of the same class from different domains are mapped nearby. This motivates our use of class centroid alignment in UDA, following the approach in [16].

To implement the class centroid alignment, pseudo labels are first assigned using a target classifier F , after which centroids are computed for both labeled and pseudo-labeled samples. The centroid alignment objective is defined as:

$$\mathcal{L}_{CA}(\mathcal{X}_S, \mathcal{Y}_S, \mathcal{X}_T, \mathcal{Y}_T) = \sum_{k=1}^K \phi(C_S^k, C_T^k), \quad (17)$$

where C_S^k and C_T^k are the centroids of class k in the source and target domains, respectively. The distance measure $\phi(\cdot, \cdot)$ is defined as the squared Euclidean distance $\phi(x, x') = \|x - x'\|^2$. By minimizing the distance between centroids across domains, we ensure that features of the same class are mapped nearby.

2.4. Implementation Details

The overall framework of our final model is illustrated in Figure 2. After extracting features from the input, we

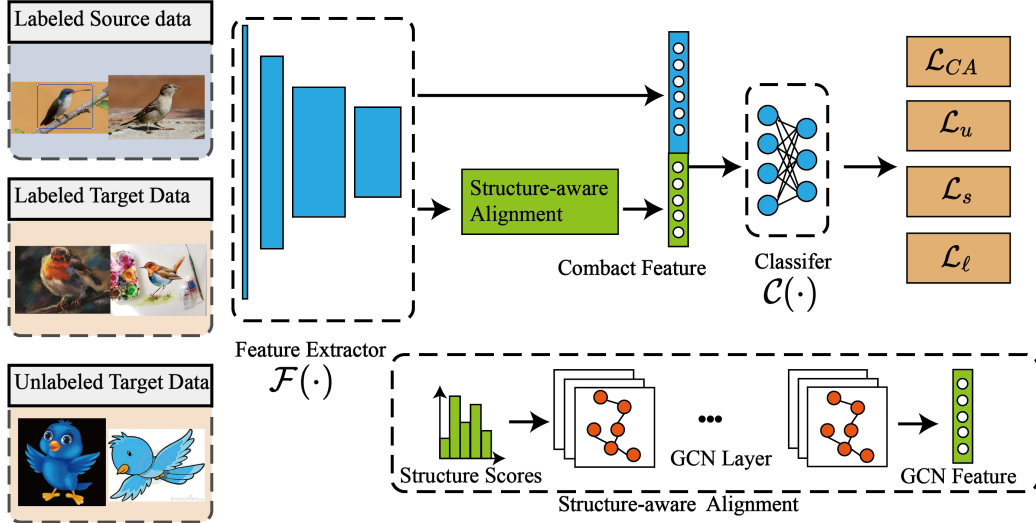


Figure 2. Overall framework of our model.

compute the structural score using Structure-aware Alignment and extract structural features through Graph Convolutional Networks (GCN). These features are then concatenated with the original features to create the final feature representation. Finally, we utilize the final loss for convergence, which is defined as follows:

$$\begin{aligned} \mathcal{L}_{AGLP} &= \mathcal{L}_{CDACSLA} + \beta \mathcal{L}_{CA}(\mathcal{X}_S, \mathcal{Y}_S, \mathcal{X}_T, \mathcal{Y}_T) \\ &= \tilde{\mathcal{L}}_s(g|S) + \mathcal{L}_{CE} + \mathcal{L}_{AAC} + \mathcal{L}_{PL} + \mathcal{L}_{Con} + \beta \mathcal{L}_{CA}(\mathcal{X}_S, \mathcal{Y}_S, \mathcal{X}_T, \mathcal{Y}_T) \end{aligned} \quad (18)$$

where β is a hyperparameter, which is typically set to 1 in our experiments.

3. Experiments

3.1. Experiment Datasets

We evaluate our proposed AGLP framework on two SSSDA benchmarks: Office-Home [23] and DomainNet [18].

Office-Home [23] is an object recognition benchmark consisting of 15,500 images from 65 classes across four domains: Art (A), Clipart (C), Product (P), and Real World (R). The domain shift primarily results from variations in image styles and perspectives.

DomainNet [18] is a dataset featuring common objects across six different domains, including 345 classes such as bracelets, airplanes, birds, and cellos. The domains include Clipart, which contains clipart images; Real, comprising photographs and real-world images; Sketch, featuring sketches of tangible objects; Infograph, containing infographics with specific objects; Painting, showcasing artistic representations; and Quickdraw, which consists of

Algorithm 1: AGLP algorithm.

Input:

- 1) Source domain data $S = \{(x_i^s, y_i^s)\}_{i=1}^{N_s}$
- 2) Unlabeled target data $U = \{(x_i^u)\}_{i=1}^{N_u}$
- 3) Labeled target data $L = \{(x_i^l, y_i^l)\}_{i=1}^{N_l}$
- 4) Feature extractor $\mathcal{F}(\cdot)$
- 5) Classifier $\mathcal{C}(\cdot)$
- 6) GCN network

- 1 Initialize all parameters
 - 3 **for** $l \leftarrow 0$ to L **do**
 - 5 Randomly sample a batch of data from $\mathcal{S}, \mathcal{U}, \mathcal{L}$.
 - 7 Use $\mathcal{F}(\cdot)$ to extract features and obtain G as shown in Eq. 15.
 - 9 Obtain the structural information feature \hat{A} by passing G through the DSA in Eq. 16.
 - 11 Concatenate \hat{A} with G and feed the combined features into $\mathcal{C}(\cdot)$.
 - 13 Train $\mathcal{C}(\cdot)$ and $\mathcal{F}(\cdot)$ using the losses $\tilde{\mathcal{L}}_s(g|S), \mathcal{L}_{CE}, \mathcal{L}_{AAC}, \mathcal{L}_{PL}, \mathcal{L}_{Con}$, and \mathcal{L}_{CA} .
 - 14 **end**
 - 15 **return** $\mathcal{C}(\cdot), \mathcal{F}(\cdot)$
-

drawings made by players worldwide. In line with prior works [11, 25, 26], we select four domains—Clipart (C), Painting (P), Real (R), and Sketch (S)—to conduct experiments on 126 classes. For dataset processing, we employ the same sampling strategy for the training and validation sets as utilized in recent studies [11, 25, 26]. Each dataset is evaluated through both one-pass and three-pass experiments.

Method	A→C	A→P	A→R	C→A	C→P	C→R	P→A	P→C	P→R	R→A	R→C	R→P	Avg
S+T	54.0	73.1	74.2	57.6	72.3	68.3	63.5	53.8	73.1	67.8	55.7	80.8	66.2
DANN[3]	54.7	68.3	73.8	55.1	67.5	67.1	56.6	51.8	69.2	65.2	57.3	75.5	63.5
ENT[4]	61.3	79.5	79.1	64.7	79.1	70.2	62.6	85.7	71.9	73.4	66.4	86.2	74.0
APE[8]	63.9	81.1	80.2	66.6	79.9	76.8	67.1	65.2	82.0	74.0	70.4	87.7	75.7
DECOTA[26]	64.0	81.8	80.5	68.0	83.2	79.0	69.9	68.0	82.1	74.0	70.4	87.7	75.7
MME[20]	63.6	79.0	79.7	67.2	79.6	76.6	65.5	64.6	80.1	71.3	64.6	85.5	73.1
MME SLA[27]	65.9	81.1	80.5	69.2	81.9	79.4	69.7	67.4	81.9	74.7	68.4	87.4	75.6
CDAC[11]	66.7	79.0	83.6	66.7	78.0	80.0	64.1	67.2	86.2	68.7	69.7	86.2	74.7
CDAC SLA[27]	65.6	81.4	81.1	68.2	82.1	80.1	67.7	68.9	82.6	69.0	69.7	86.3	75.2
AGLP(Ours)	68.9	85.1	87.2	70.3	82.1	81.0	70.3	71.3	88.2	71.3	70.3	85.6	77.6

Table 1. In the 3-Shot comparison experiments conducted on the Office-Home dataset, the best results are highlighted in bold.

Method	A→C	A→P	A→R	C→A	C→P	C→R	P→A	P→C	P→R	R→A	R→C	R→P	Avg
S+T	50.9	69.8	73.8	56.3	68.1	70.0	57.2	48.3	74.4	66.2	52.1	78.6	63.8
DANN[3]	52.3	67.9	73.9	54.1	66.8	69.2	55.7	51.9	68.4	64.5	53.1	74.8	62.7
ENT[4]	52.9	75.0	76.7	63.2	73.6	70.4	53.6	81.9	67.9	72.5	60.7	81.6	68.9
APE[8]	53.9	76.1	75.2	63.6	69.8	72.3	58.3	78.6	72.5	71.3	56.0	79.4	64.8
DECOTA[26]	42.1	68.5	72.6	60.3	70.4	71.3	48.8	76.9	71.2	70.7	60.0	79.4	64.8
MME[20]	59.6	75.5	77.8	65.7	74.5	74.8	64.7	57.4	79.2	71.2	61.9	82.8	70.4
MME SLA[27]	62.1	76.3	78.6	67.5	77.1	75.1	66.7	59.9	80.0	72.9	64.1	83.8	72.0
CDAC[11]	61.2	75.9	78.5	64.5	75.1	75.3	64.6	59.3	80.0	72.7	61.9	83.1	71.0
CDAC SLA[27]	61.4	77.8	79.2	66.9	76.2	75.9	66.3	60.6	80.5	71.6	65.6	84.3	72.2
AGLP(Ours)	66.2	84.1	85.6	67.2	75.5	76.8	68.2	62.1	84.6	71.9	69.7	84.6	74.7

Table 2. In the 1-Shot comparison experiments conducted on the Office-Home dataset, the best results are highlighted in bold.

3.2. Comparison Methods and Settings

We compare our results with several baselines, including S+T, DANN [3], ENT [4], APE [8], DECOTA [26], MME [20], MME SLA [27], CDAC [11], and CDAC SLA [27]. Among these, S+T serves as the baseline method for SSDA, where training involves only source data and labeled target data. DANN is a classical unsupervised domain adaptation method, replicated here by training on additional labeled target data. ENT is the standard entropy minimization method originally designed for semi-supervised learning.

Our framework can be applied to various state-of-the-art methods. To verify the effectiveness of our approach, we select CDAC SLA [27] as the baseline. For a fair comparison, we adopt ResNet34 [6] as the backbone network. The backbone network is pre-trained on the ImageNet1K dataset [2], and we follow the same model architecture, batch size, learning rate scheduler, optimizer, weight decay, and initial-

ization strategies as in previous works [11, 20]. For MME and CDAC, we use the same hyperparameters as recommended in their original papers. For SLA, we set the mixing ratio α to 0.3 and the temperature parameter T to 0.6. The update interval is set to 500. For MME, the warmup parameter W is 500 on Office-Home and 3000 on DomainNet, while for CDAC, W is 2000 on Office-Home and 5000 on DomainNet. After the warmup phase, we reset the learning rate scheduler to allow label adaptation loss updates at a higher learning rate. All hyper-parameters are fine-tuned through a validation process. For each sub-task, we conduct three experiments. The hyper-parameters for the other comparative models are kept identical to those in their original papers.

The parameters we use in the structure alignment module are as follows: the input channels for the GCN are set to 1000, with hidden channels set to 256 and dropout set to 0.2. The output channels are configured to 200 for the

Office-Home dataset and 25 for DomainNet. The number of GCN layers is set to 4 for the Office-Home dataset and 8 for DomainNet. Additionally, the hyper-parameter β in the class centroid alignment section is uniformly set to 1 throughout the paper. A robustness analysis of these parameters is provided in the supplementary materials.

3.3. Comparative Experiments

Comparative Experiments on Office-Home: We conducted 1-Shot and 3-Shot experiments on the Office-Home dataset, with results summarized in Table. 1 and Table. 2. In the Office-Home 3-Shot experiment, our method, AGLP, demonstrated excellent performance across multiple transfer tasks, achieving an average accuracy of 77.6%, surpassing all other methods, including the baseline CDAC SLA. In the more stringent Office-Home 1-Shot setting, AGLP maintained its lead with an average accuracy of 74.7%, showcasing robust performance even under data-scarce conditions. The AGLP method exhibited significant improvements in both the 3-Shot and 1-Shot experiments, exceeding the previous state-of-the-art baseline by 2.4% and 1.8% in accuracy, respectively. These results affirm the effectiveness of our approach in semi-supervised domain adaptation tasks across varying data availability scenarios.

Comparative Experiments on DomainNet: To further validate the performance of our model, we conducted 1-Shot and 3-Shot experiments on the larger and more complex DomainNet dataset, with results summarized in Table. 3 and Table. 4. Our model achieved accuracies of 75.3% and 77.3%, outperforming all comparative methods. Specifically, compared to the baseline (CDAC SLA), the model’s accuracy improved by 0.5% in the 1-Shot experiment and by 0.8% in the 3-Shot experiment. It is noteworthy that due to the larger and more complex nature of the DomainNet dataset, the performance improvements were less pronounced compared to those observed in Office-Home. Nevertheless, these results demonstrate that our model maintains strong performance even on more challenging datasets.

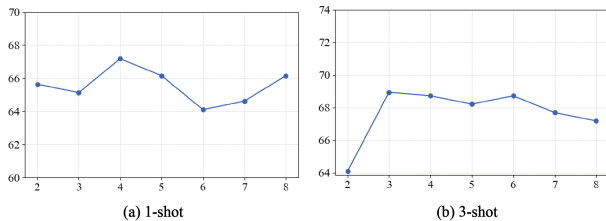


Figure 3. In the domain adaptation experiment of Office-Home 3-Shot A→C, we conducted a parameter analysis by varying the output channels.

Method	R→C	R→P	P→C	C→S	S→P	R→S	P→R	Avg.
S+T	60.0	62.2	59.4	55.0	59.5	50.1	73.9	60.0
DANN[3]	59.8	62.8	59.6	55.4	59.9	54.9	72.2	60.7
ENT[4]	71.0	69.2	71.1	60.0	62.1	61.1	78.6	67.6
APE[8]	76.6	72.1	76.7	63.1	66.1	67.8	79.4	71.7
DECOTA[26]	80.4	75.2	78.7	68.6	72.7	71.9	81.5	75.6
MME[20]	72.2	69.7	71.7	61.8	66.8	61.9	78.5	68.9
MME SLA[27]	73.3	70.1	72.7	63.4	67.3	63.9	79.6	70.0
CDAC[11]	79.6	75.1	79.3	69.9	73.4	72.5	81.9	76.0
CDAC SLA[27]	80.9	75.2	80.2	70.8	72.4	73.5	82.5	76.5
AGLP(Ours)	82.0	76.4	81.4	71.6	73.4	73.5	82.6	77.3

Table 3. In the 3-Shot comparison experiments conducted on the DomainNet dataset, the best results are highlighted in bold.

Method	R→C	R→P	P→C	C→S	S→P	R→S	P→R	Avg.
S+T	55.6	60.6	56.8	50.8	56.0	46.3	71.8	56.9
DANN[3]	58.2	61.4	56.3	52.8	57.4	52.2	70.3	58.4
ENT[4]	65.2	65.9	65.4	54.6	59.7	52.1	75.0	62.6
APE[8]	70.4	70.8	72.9	56.7	64.5	63.0	76.6	67.6
DECOTA[26]	79.1	74.9	76.9	65.1	72.0	69.7	79.6	73.9
MME[20]	70.0	67.7	69.0	56.3	64.8	61.0	76.1	66.4
MME SLA[27]	71.8	68.2	70.4	59.3	64.9	61.8	77.2	68.8
CDAC[11]	77.4	74.2	75.5	67.6	71.0	69.2	80.4	73.6
CDAC SLA[27]	79.2	75.2	77.2	68.1	71.7	71.7	80.4	74.8
AGLP(Ours)	80.1	75.7	77.2	68.9	71.9	72.0	81.0	75.3

Table 4. In the 1-Shot comparison experiments conducted on the DomainNet dataset, the best results are highlighted in bold.

3.4. Further Performance Analysis

3.4.1 Ablation Study

To further validate the effectiveness of our model, we conducted an ablation study on Office-Home 3-Shot, as shown in Table 5. In this study, SAA refers to structure-aware alignment, and CA denotes class centroid alignment. As presented in Table 5, each component provides significant improvements over the baseline (CDAC SLA), although the enhancement from CA is less pronounced. This may be attributed to CA primarily optimizing the scores of structure-aware alignment. When both components are utilized together, optimal performance is achieved. Overall, our improvements are evidently effective and can be transferred to other models.

3.4.2 Visualization Analysis

To more intuitively validate our model, we conducted various analyses during the Office-Home 3-Shot A→C domain adaptation experiment, including t-SNE dimensionality reduction visualization, confusion matrix evaluation, loss convergence, and accuracy comparison.

Confusion Matrix: The confusion matrix comparison in

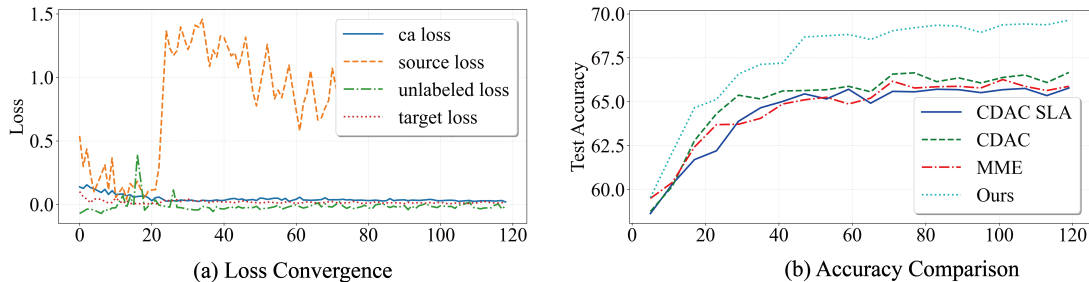


Figure 4. (a) illustrates the convergence behavior of the four loss functions in our model during the Office-Home 3-Shot A→C domain adaptation experiment. (b) depicts the accuracy variations of the four models throughout the same experiment.

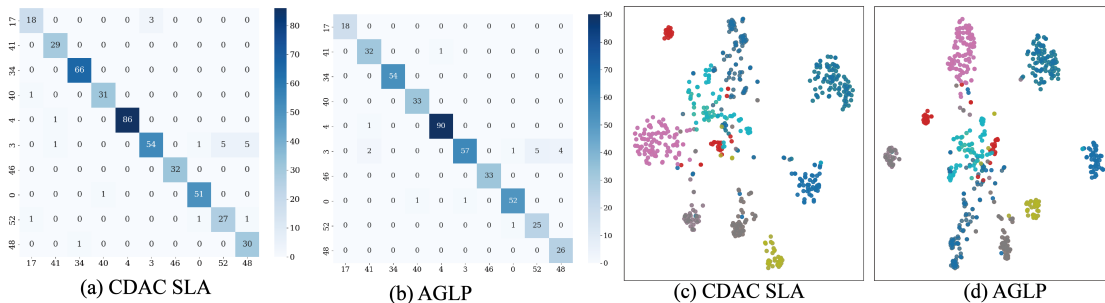


Figure 5. In the Office-Home 3-Shot A→C domain adaptation experiment, the confusion matrix and visualization analysis were computed by randomly selecting 10 classes from the dataset.

Method	Method		Domain					Avg.
	<i>baseline</i>	SAA	CA	A→C	C→P	P→R	R→A	
	✓	✗	✗	65.6	82.1	82.6	69.0	74.8
	✓	✓	✗	68.7	82.2	86.5	70.2	76.9
	✓	✗	✓	67.4	81.7	85.4	69.8	76.1
AGLP(Ours)	✓	✓	✓	68.9	82.1	88.2	71.3	77.6

Table 5. Ablation experiments were conducted on the Office-Home 3-Shot experiment, with the best results indicated in bold.

Figure 5 (a) and (b) highlights the performance of our model against the baseline (CDAC SLA). We calculated the confusion matrix for the 10 selected categories based on the test samples, providing a detailed breakdown of the model’s performance across each category. Not only does our approach exhibit superior classification accuracy, but it also highlights the robustness and reliability of our model in comparison to the baseline approach.

Dimensionality Reduction Visualization: As shown in Figure 5 (c) and (d), we compared MME SLA[27], CDAC[11], CDAC SLA[27], and our model. We randomly selected 10 categories from the 65 categories in Office-Home and extracted features using the trained model, subsequently reducing them to a two-dimensional space using t-SNE. Our model exhibits better clustering of sample fea-

tures, demonstrating improved domain adaptation performance.

Loss Convergence: The loss convergence results are depicted in Figure 4 (a). Here, CA loss represents our improvement \mathcal{L}_{CA} , Source loss denotes $\tilde{\mathcal{L}}_s(g|S)$, Target loss corresponds to \mathcal{L}_{CE} , and Unlabeled loss represents \mathcal{L}_u . Our model demonstrates rapid convergence during training. Notably, $\tilde{\mathcal{L}}_s(g|S)$ experiences a spike due to warmup but subsequently converges effectively.

Test Accuracy Comparison: The accuracy variation results, shown in Figure 4 (b), compare our model with MME SLA[27], CDAC, and CDAC SLA. Our model consistently maintains superior accuracy, confirming its excellent performance.

4. Conclusion

In this paper, we propose a novel method by leveraging graph structure information in a unified network for semi-supervised domain adaptation. Our model introduces a class alignment loss to achieve this goal and employs a moving centroid strategy to mitigate the influence of incorrect pseudo-labels. To match source and target domain distribution robustly, we design an effective structure data alignment mechanism for SSDA. By modeling this alignment mechanism, the deep network can generate domain-invariant and highly discriminative semantic representa-

tions. Experiments on standard domain adaptation datasets verify the effectiveness of the proposed model.

References

- [1] David Berthelot, Rebecca Roelofs, Kihyuk Sohn, Nicholas Carlini, and Alex Kurakin. Adamatch: A unified approach to semi-supervised learning and domain adaptation. *arXiv preprint arXiv:2106.04732*, 2021. [1](#), [2](#)
- [2] Jia Deng, Wei Dong, Richard Socher, Li-Jia Li, Kai Li, and Li Fei-Fei. Imagenet: A large-scale hierarchical image database. In *CVPR*, pages 248–255. Ieee, 2009. [6](#)
- [3] Yaroslav Ganin, Evgeniya Ustinova, Hana Ajakan, Pascal Germain, Hugo Larochelle, François Laviolette, Mario March, and Victor Lempitsky. Domain-adversarial training of neural networks. *Journal of Machine Learning Research*, 17(59):1–35, 2016. [6](#), [7](#)
- [4] Yves Grandvalet and Yoshua Bengio. Semi-supervised learning by entropy minimization. *NIPS*, 17, 2004. [6](#), [7](#)
- [5] Gewen He, Xiaofeng Liu, Fangfang Fan, and Jane You. Classification-aware semi-supervised domain adaptation. In *CVPR*, pages 964–965, 2020. [2](#)
- [6] Kaiming He, Xiangyu Zhang, Shaoqing Ren, and Jian Sun. Deep residual learning for image recognition. In *CVPR*, pages 770–778, 2016. [6](#)
- [7] Pin Jiang, Aming Wu, Yahong Han, Yunfeng Shao, Meiyu Qi, and Bingshuai Li. Bidirectional adversarial training for semi-supervised domain adaptation. In *IJCAI*, pages 934–940, 2020. [1](#)
- [8] Taekyung Kim and Changick Kim. Attract, perturb, and explore: Learning a feature alignment network for semi-supervised domain adaptation. In *ECCV*, pages 591–607. Springer, 2020. [6](#), [7](#)
- [9] Thomas N Kipf and Max Welling. Semi-supervised classification with graph convolutional networks. *arXiv preprint arXiv:1609.02907*, 2016. [4](#)
- [10] Da Li and Timothy Hospedales. Online meta-learning for multi-source and semi-supervised domain adaptation. In *ECCV*, pages 382–403. Springer, 2020. [2](#)
- [11] Jichang Li, Guanbin Li, Yemin Shi, and Yizhou Yu. Cross-domain adaptive clustering for semi-supervised domain adaptation. In *CVPR*, pages 2505–2514, 2021. [2](#), [5](#), [6](#), [7](#), [8](#)
- [12] Limin Li and Zhenyue Zhang. Semi-supervised domain adaptation by covariance matching. *TPAMI*, 41(11):2724–2739, 2018. [1](#)
- [13] Wuyang Li, Jie Liu, Bo Han, and Yixuan Yuan. Adjustment and alignment for unbiased open set domain adaptation. In *CVPR*, pages 24110–24119, 2023. [4](#)
- [14] Zhenghua Li, Xue Peng, Min Zhang, Rui Wang, and Luo Si. Semi-supervised domain adaptation for dependency parsing. In *ACL*, pages 2386–2395, 2019. [1](#)
- [15] Mattia Litrico, Alessio Del Bue, and Pietro Morerio. Guiding pseudo-labels with uncertainty estimation for source-free unsupervised domain adaptation. In *CVPR*, pages 7640–7650, 2023. [2](#)
- [16] Xinhong Ma, Tianzhu Zhang, and Changsheng Xu. Gcan: Graph convolutional adversarial network for unsupervised domain adaptation. In *CVPR*, pages 8266–8276, 2019. [4](#)
- [17] Poojan Oza, Vishwanath A Sindagi, Vibashan Vishnukumar Sharmini, and Vishal M Patel. Unsupervised domain adaptation of object detectors: A survey. *IEEE TPAMI*, 2023. [4](#)
- [18] Xingchao Peng, Qinxun Bai, Xide Xia, Zijun Huang, Kate Saenko, and Bo Wang. Moment matching for multi-source domain adaptation. In *ICCV*, pages 1406–1415, 2019. [1](#), [5](#)
- [19] Lei Qi, Hongpeng Yang, Yinghuan Shi, and Xin Geng. Multitmatch: Multi-task learning for semi-supervised domain generalization. *ACM Transactions on Multimedia Computing, Communications and Applications*, 20(6):1–21, 2024. [1](#)
- [20] Kuniaki Saito, Donghyun Kim, Stan Sclaroff, Trevor Darrell, and Kate Saenko. Semi-supervised domain adaptation via minimax entropy. In *ICCV*, pages 8050–8058, 2019. [2](#), [6](#), [7](#)
- [21] Ankit Singh. Clda: Contrastive learning for semi-supervised domain adaptation. *NIPS*, 34:5089–5101, 2021. [1](#)
- [22] Yiyu Sun, Yaojie Liu, Xiaoming Liu, Yixuan Li, and Wen-Sheng Chu. Rethinking domain generalization for face anti-spoofing: Separability and alignment. In *CVPR*, pages 24563–24574, 2023. [4](#)
- [23] Hemanth Venkateswara, Jose Eusebio, Shayok Chakraborty, and Sethuraman Panchanathan. Deep hashing network for unsupervised domain adaptation. In *CVPR*, pages 5018–5027, 2017. [1](#), [5](#)
- [24] Yan Wang, Junbo Yin, Wei Li, Pascal Frossard, Ruigang Yang, and Jianbing Shen. Ssda3d: Semi-supervised domain adaptation for 3d object detection from point cloud. In *AAAI*, pages 2707–2715, 2023. [2](#)
- [25] Zizheng Yan, Yushuang Wu, Guanbin Li, Yipeng Qin, Xiaoguang Han, and Shuguang Cui. Multi-level consistency learning for semi-supervised domain adaptation. *arXiv preprint arXiv:2205.04066*, 2022. [5](#)
- [26] Luyu Yang, Yan Wang, Mingfei Gao, Abhinav Shrivastava, Kilian Q Weinberger, Wei-Lun Chao, and Ser-Nam Lim. Deep co-training with task decomposition for semi-supervised domain adaptation. In *ICCV*, pages 8906–8916, 2021. [5](#), [6](#), [7](#)
- [27] Yu-Chu Yu and Hsuan-Tien Lin. Semi-supervised domain adaptation with source label adaptation. In *CVPR*, pages 24100–24109, 2023. [2](#), [3](#), [6](#), [7](#), [8](#)
- [28] Zhongqi Yue, Qianru Sun, and Hanwang Zhang. Make the u in uda matter: Invariant consistency learning for unsupervised domain adaptation. *NIPS*, 36:26991–27004, 2023. [2](#)